Journal of the Physical Society of Japan
Vol. 67, No. 10, October, 1998, pp. 3621-3629

A Model Study on Cluster Size Effects of Resonant X-Ray Emission Spectra

Tsuyoshi IDÉ* and Akio KOTANI

Institute for Solid State Physics, The University of Tokyo, 7-22-1 Roppongi, Minato-ku, Tokyo 106-8666

(Received May 14, 1998)

Cluster size dependence of X-ray absorption spectra (XAS), X-ray photoemission spectra (XPS), and resonant X-ray emission spectra (RXES) are theoretically studied with a one-dimensional *d-p* model, which describes qualitatively effects of translational symmetry for nominally d^0 (or f^0) compounds such as TiO_2 (CeO_2). It is shown that RXES depends more sensitively on the cluster size than XAS and XPS, so that RXES is a useful probe in studying the duality between itinerant and localized characters of $3d$ or $4f$ electrons. From results calculated by changing the cluster size and parameter values such as *p-d* hybridization strength, *d-d* Coulomb interaction etc., it is explained why the experimental Ce $4f$-$3d$ RXES of CeO_2 is well reproduced by calculations with a single-cation impurity Anderson model, but the Ti $3d$-$2p$ RXES of TiO_2 is not well reproduced.

KEYWORDS: resonant X-ray emission, one dimensional *d-p* model, multi-site cluster, Lanczos method

§1. Introduction

It has been accepted that one of key concepts to understand electronic properties of strongly correlated systems involving $3d$ or $4f$ orbitals is the duality between localized and itinerant natures of electrons. High-energy spectroscopies have played vital roles to investigate these systems. It is reasonable that X-ray photoemission spectroscopy (XPS) and X-ray absorption spectroscopy (XAS) of these systems are considerably well described with the Anderson impurity model including a single cation,[1] because a completely localized core electron is involved in these spectroscopies and the core hole acts as a localized attractive potential acting on the $3d$ or $4f$ electrons. However, since van Veenendaal *et al.* demonstrated importance of nonlocal screening effects in analyses of metal $2p$ XPS for NiO[2] and high T_c compounds,[3] those phenomena in which the itinerant property of $3d$ electrons plays an essential role have attracted much attention in this field.

Since the advent of the third generation synchrotron radiation sources, a number of experimental investigations on resonant X-ray emission spectroscopy (RXES) have been performed. RXES is the second order optical process where a core electron is photoexcited to levels near the absorption threshold. In intermediate states of the RXES process, valence electrons feel a localized core hole potential, but in the final state their Hamiltonian restores the translational symmetry. Thus their itinerant nature as well as localized nature should be strongly reflected on the spectral shape of RXES, despite of its site-selectivity. Furthermore, RXES is very sensitive to electron dynamics and relaxation of the intermediate state through the coherent second order optical process. In this sense RXES is one of the most adequate probes to "see" the strongly correlated systems involving $3d$ or $4f$ electrons. Our main motivation is to investigate how their itinerancy appears itself in the spectra. It necessarily needs an extended cluster model beyond the single-cation impurity limit.

Experimental data of RXES for graphite,[4] Si[5] and diamond[6] have shown that the wave vector conservation rule, which is a mathematical consequence of the itinerancy of valence electrons, plays an important role in RXES spectra. For transition metal compounds such as TiO_2[7] and $FeTiO_3$[8] remarkable spectral features have been observed: in addition to inelastic X-ray scattering peaks whose emitted photon energy moves in parallel with the incident photon energy, giant inelastic spectra are observed at nearly the same energy position for any incident photon energy, and they are connected smoothly to the line shape of normal X-ray emission spectroscopy (NXES) as the incident photon energy increases well above the absorption threshold.

We expect that a source of the latter kind of features, which is hard to understand with the single-cation impurity model, is the itinerancy of $3d$ electrons. We would like to study how the translational symmetry of crystals modifies RXES spectra, and to give a physical picture of the X-ray emission process. To accomplish this, we adopt a one-dimensional *d-p* model without orbital degeneracies as a minimal model having explicit translational symmetry.

The structure of this paper is as follows: in §2 we explain the model used. In §3 we give results of numerical calculations on XAS, XPS, RXES and NXES for TiO_2-like and CeO_2-like parameters. In §4 physical interpretations for these spectra are presented, paying attention to role of the wave vector conservation rule. In the last section, we will give a brief summary of the present study.

* E-mail: ide@kodama.issp.u-tokyo.ac.jp

§2. Description of the Model

2.1 Hamiltonian

We consider the following one-dimensional (1D) d-p Hamiltonian as a model of TiO_2:

$$H = H_0 + H_1 + V_{dc} + V_{dd} + H_{\rm core}, \tag{2.1}$$

where

$$H_0 = \sum_{l,\sigma} \left[(\Delta + \varepsilon_p)\, d^\dagger_{l\sigma} d_{l\sigma} + \varepsilon_p\, p^\dagger_{l\sigma} p_{l\sigma} \right], \tag{2.2a}$$

$$H_1 = \sum_{\langle i,j \rangle} \sum_{\sigma} \left[v\, d^\dagger_{i\sigma} p_{j\sigma} + v^* p^\dagger_{j\sigma} d_{i\sigma} \right], \tag{2.2b}$$

$$V_{dc} = -U_{dc} \sum_{l} \left(\sum_{\sigma} d^\dagger_{l\sigma} d_{l\sigma} \right) \left(\sum_{\sigma'} c_{l\sigma'} c^\dagger_{l\sigma'} \right), \tag{2.2c}$$

$$V_{dd} = U_{dd} \sum_{l} d^\dagger_{l\uparrow} d_{l\uparrow} d^\dagger_{l\downarrow} d_{l\downarrow}, \tag{2.2d}$$

and

$$H_{\rm core} = \sum_{l,\sigma} \varepsilon_c\, c^\dagger_{l\sigma} c_{l\sigma}. \tag{2.2e}$$

In the above equations, $d^\dagger_{l\sigma}$ ($p^\dagger_{l\sigma}$) is a creation operator of σ spin electron on the d (p) site in l-th unit cell, Δ is the charge-transfer energy between d and p orbitals, U_{dd} is the on-site d-d Coulomb correlation energy, and U_{dc} is the intra-atomic core hole potential. $c^\dagger_{l\sigma}$ ($c_{l\sigma}$) is a creation (annihilation) operator of core electrons. Geometry of the system is shown in Fig. 1. We set the number of valence electrons in the ground state as $2N$ for $d_M p_N$ system, assuming the z-component of the total spin $S_z = 0$.

The d_1p_2 cluster with the *open boundary condition* (Fig. 1(a)) is used as a reference system representing the smallest cluster with a single cation (or the Anderson impurity model), and large cluster effects are studied using $d_N p_N$ clusters with the *periodic boundary condition* (Fig. 1(b)) by comparing the results calculated with different N (also with the d_1p_2 system).

H_1 describes the nearest neighbor d-p hopping process. Although we do not explicitly consider orbital degeneracies and the point group symmetry of crystals, in order to take into account their effects to some extent, the d-p hopping energy v is estimated by the equation

$$v = \frac{1}{2}\sqrt{4V(e_g)^2 + 6V(t_{2g})^2}, \tag{2.3}$$

where $V(e_g)$ and $V(t_{2g})$ are hybridization strengths of TiO_6 cluster model.[9] In Appendix we explain the way of estimating the parameter v.

Okada and Kotani[9] used parameter values $V(e_g) = 3.0$ and $V(t_{2g}) = -1.5$, from which we have $v = 3.5$ (in units of eV). Other parameters are chosen to be the same as their estimation: $\Delta = 4.0$, $U_{dd} = 4.0$ and $U_{dc} = 6.0$ (in eV). These will be referred to as "TiO_2-like" parameters.

$H_{\rm core}$ describes the core level state. We regard the core orbital as that of Ti $2p$, and d (p) as Ti $3d$ (O $2p$) for TiO_2-like calculations. The spin-orbit coupling is omitted for simplicity. Note that core orbitals of all different d-sites participate in the RXES process. Therefore we must not fix the core hole to a single site (see discussions in §2.2 and §4.3).

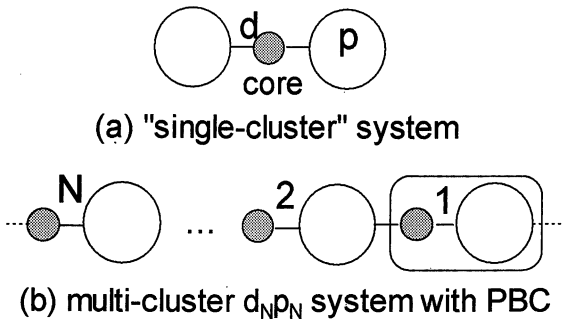

Fig. 1. Geometry of the system. Closed circles represent d and core orbitals, and open circles represent p orbitals. The round rectangle indicates a unit cluster of the system. (a) d_1p_2 cluster with the open boundary condition used as a reference system representing the smallest cluster with a single cation. (b) Multi-cluster system with the periodic boundary condition.

The Hamiltonian described above can also be used for Ce $4f$-$3d$ RXES spectra of a "CeO_2-like" system by regarding d, p and c as Ce $4f$, O $2p$ and Ce $3d$ orbitals, respectively. Since the Anderson impurity model with local $SO(3)$ symmetry has well reproduced Ce $3d$ XAS spectra,[10,11] the f-p hybridization strength mapped onto 1D Hamiltonian should be simply given by $v = \sqrt{14}V/2$, where 14 is the degeneracy of $4f$ state. Considering the results by Jo and Kotani[10] and Nakazawa *et al.*,[11] for "CeO_2-like" calculations we use a parameter set of $\Delta = 1.5$, $U_{ff} = 10.0$, $U_{fc} = 13.0$, and $v = 1.5$ (in eV).

2.2 Spectral functions

For our 1D model the transition operators of the photon absorption and emission process in the dipole approximation are given by

$$T_1 = \sum_{l} {\rm e}^{{\rm i}q_1 l} \sum_{\sigma} d^\dagger_{l\sigma} c_{l\sigma} \cdot b_{q_1} \tag{2.4}$$

and

$$T_2 = \sum_{l} {\rm e}^{-{\rm i}q_2 l} \sum_{\sigma} c^\dagger_{l\sigma} d_{l\sigma} \cdot b^\dagger_{q_2}, \tag{2.5}$$

where q_1 is the wave number of an incident photon and q_2 an emitted photon, b_{q_1} and $b^\dagger_{q_2}$ are operators of photon annihilation and creation, respectively.[12] With these operators the transition amplitude of the RXES process is

$$\begin{aligned} U_{g\to f}(\Omega) &= \langle f | T_2 G(\Omega + {\rm i}\Gamma_m) T_1 | g \rangle \\ &= \sum_{l\sigma} {\rm e}^{{\rm i}(q_1 - q_2)l} \langle f | c^\dagger_{l\sigma} d_{l\sigma} G(\Omega + {\rm i}\Gamma_m) d^\dagger_{l\sigma} c_{l\sigma} | g \rangle, \end{aligned}$$

where $|g\rangle$ is the ground state having a photon of q_1, $|f\rangle$ is a final state having a photon of q_2, and G is the resolvent operator defined by $G(z) = (z - E_g - H)^{-1}$, E_g and Ω being the ground state energy and the incident photon energy, respectively. For $3d$- or $4f$- systems the damping Γ_m mainly comes from the Auger decay process of the core hole, so that we disregard the phonon relaxation process in the intermediate state.[13]

Under the periodic boundary condition, because of translational invariance of the Hamiltonian and the re-

solvent operator, both the initial and final states are irreducible representations of the translation group, and the wave vector is conserved between these two states, regardless of existence of U_{dd} or U_{dc}. Then the amplitude is written as

$$U_{g\to f}(\Omega) = N\delta(q_1 + K_g - q_2 - K_f) \times \sum_\sigma \langle f|c^\dagger_{0\sigma} d_{0\sigma} G(\Omega + \mathrm{i}\Gamma_m) d^\dagger_{0\sigma} c_{0\sigma}|g\rangle. \quad (2.6)$$

The factor before the summation indicates total wave vector conservation rule.[14] If the core hole is fixed on a single site, we do not have the conservation rule. In contrast to the first-order optical process, spatial coherence in this sense is essential to understand RXES spectra.[15]

As van Veenendaal and Carra pointed out within the independent quasi-particle limit,[16] the amplitude of the elastic scattering is proportional to N, which is the number of unit clusters, and therefore the intensity is of the order N^2 if the Bragg condition is satisfied.[17] In the present paper, however, we concentrate our attention to only inelastic lines from now on.

After all, RXES spectral function is calculated by

$$F_{\mathrm{RXES}}(\Omega, \omega) = \frac{1}{N} \sum_{f\neq g} |U_{g\to f}(\Omega)|^2 \delta(\omega - \Omega + E_f - E_g), \quad (2.7)$$

where ω is the emitted photon energy and we introduce the normalization factor $1/N$ in order to compare systems of different cluster size. The photon wave numbers q_1 and q_2 in $U_{g\to f}$ are taken approximately as zero.

In the X-ray absorption process, the transition amplitude is $\langle m|T_1|g\rangle$ as usual, $|m\rangle$ denoting a photo-excited state with a core hole. Note that for XAS to fix the core hole site is exactly justified. The proof is as follows: for periodic systems a real number K_g exists such that $T_r(l)|g\rangle = \mathrm{e}^{\mathrm{i}K_g l}|g\rangle$, where $T_r(l)$ is a translation operator of the whole electronic system. Since the core hole site is a good quantum number in the final state of XAS, $|m\rangle$ can be written as $|\mu; l'\rangle$, l' indicating the core hole site, and therefore

$$\begin{aligned}\langle \mu; l|d^\dagger_{l\sigma} c_{l\sigma}|g\rangle &= \langle \mu; 0|T_r(l)^\dagger \cdot T_r(l) d^\dagger_{0\sigma} c_{0\sigma} T_r(l)^\dagger|g\rangle \\ &= \langle \mu; 0|d^\dagger_{0\sigma} c_{0\sigma}|g\rangle \mathrm{e}^{-\mathrm{i}K_g l},\end{aligned}$$

leading the XAS spectral function to

$$F_{\mathrm{XAS}}(\Omega) = \sum_\mu |\langle \mu; 0|d^\dagger_{0\sigma} c_{0\sigma}|g\rangle|^2 \delta(\Omega + E_\mu - E_g). \quad (2.8)$$

Normal X-ray emission spectroscopy (NXES) is the second-order optical process where a core electron is excited by the incident photon to high-energy continuum well above the absorption edge. Intermediate states of NXES are the same as final states of XPS, whose spectral function is given by

$$F_{\mathrm{XPS}}(E_B) = \sum_{\tilde\mu} |\langle \tilde\mu; 0|c_{0\sigma}|g\rangle|^2 \delta(E_B - E_{\tilde\mu} + E_g), \quad (2.9)$$

E_B being the binding energy. The energy interval of the continuum levels is so close that the momentum information of the system is hardly maintained through the NXES process. Therefore final states with any wave number are allowed. This situation is mathematically realized by fixing the core hole site. The spectral function of NXES is then given by

$$F_{\mathrm{NXES}}(\omega) = \frac{1}{N} \int \mathrm{d}\varepsilon D(\varepsilon) \sum_{f,\sigma} |\langle f|c^\dagger_{0\sigma} d_{0\sigma} G(E') c_{0\sigma}|g\rangle|^2 \times \delta(\omega + E_f + \varepsilon - \Omega - E_g), \quad (2.10)$$

where $D(\varepsilon)$ is the density of states of the continuum level ε, which will be assumed to be a constant, and $E' = \Omega + E_g - \varepsilon + \mathrm{i}\Gamma_m$. Because of the integration over ε, the spectral shape of NXES does not depend on Ω.

For numerical calculations of the spectra we use the Lanczos method.[18] Operation of the resolvent is directly calculated by so-called bi-CG algorithm.[19]

§3. Calculated Results

3.1 XPS spectra

We show XPS spectra for various cluster sizes with the TiO_2-like and the CeO_2-like parameters in Fig. 2. The calculated line spectra are convoluted with a Lorentzian function of width 1.0 eV (HWHM) corresponding to the lifetime broadening of the core hole, as well as the experimental resolution.

The XPS spectra for the TiO_2-like parameters shown in Fig. 2(a) have roughly two-peak structure with a strong main peak and a weak satellite, while a few very weak peaks come arise between them for larger cluster sizes. In the single cluster limit (d_1p_2), they correspond, respectively, to the bonding and anti-bonding final states between $\underline{c}d^0$ and $\underline{c}d^1\underline{L}$ configurations, as shown by Okada and Kotani,[9] where $\underline{c}$ represents a core hole. Also for larger cluster sizes, their characters would be essentially the same.

On the other hand, in XPS spectra for the CeO_2-like parameters (Fig. 2(b)), clear three peaks are observed, as a result of smaller value of v/U_{ff} (and also v/U_{fc}).[9] As the cluster size increases, we have slightly broader and more asymmetric shapes for the peaks in the lowest and the second-lowest binding energies. But the global structure is considerably well reproduced with the single-cation cluster f_1p_2.

3.2 XAS, RXES and NXES spectra for TiO_2-like parameters

Figures 3(a)–3(c) show XAS, NXES and RXES spectra for the TiO_2-like parameters in d_1p_2, d_3p_3 and d_6p_6 clusters, respectively. The value of Γ_m for NXES and RXES is taken as 0.4 eV, and the Lorentzian convolution with width 1.0 eV (HWHM) is made for all the spectra, as in the case of XPS.

In the case of the d_1p_2 system, inelastic RXES peaks are caused by *local* charge transfer excitations, and the emitted photon energy ω moves in parallel with the incident photon energy Ω, which is shown with the arrows. The first inelastic RXES peak corresponds to a single-electron charge transfer excitation (anti-bonding state between d^0 and $d^1\underline{L}$ configurations), while the second one mainly to a two-electrons charge transfer state with the $d^2\underline{L}^2$ configuration. In going from the d_1p_2 to d_3p_3 clusters, we find some inelastic scattering peaks which do

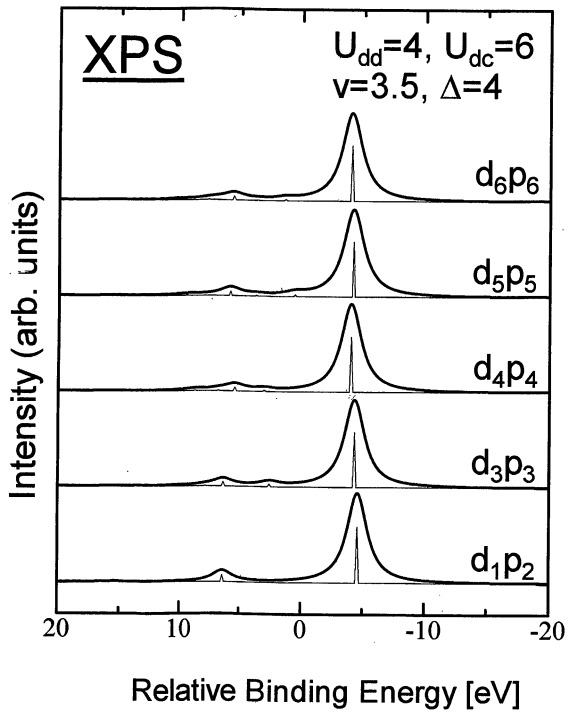

(a) TiO_2-like parameters

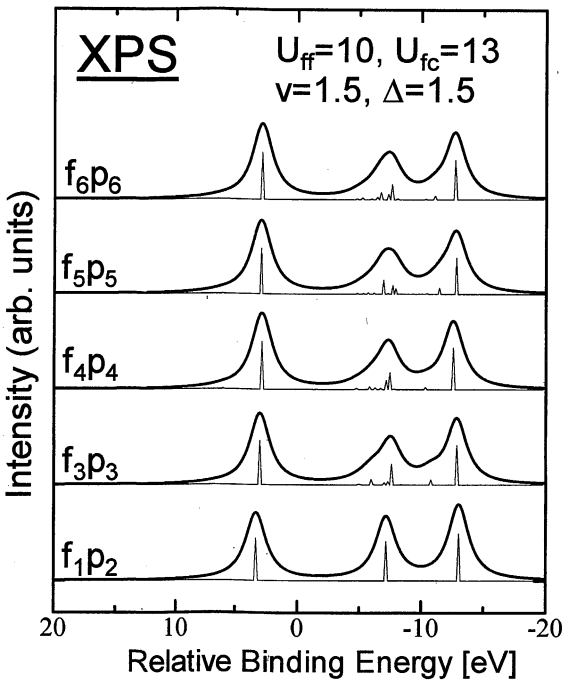

(b) CeO_2-like parameters

Fig. 2. XPS spectra calculated with various cluster sizes for (a) TiO_2-like and (b) CeO_2-like parameters.

not follow the change of the incident photon energy Ω. For the d_6p_6 cluster, the energy ω of main RXES peaks does not follow Ω but is rather constant, and it oscillates around the constant energy with the change of Ω. We denote these spectra as "*nonlocal excitation* (NLE) spectra" hereafter.

The line shape of NXES also shows, in Fig. 3, considerable dependence on the cluster size: A single peak is observed for the NXES of the d_1p_2 cluster, but it splits

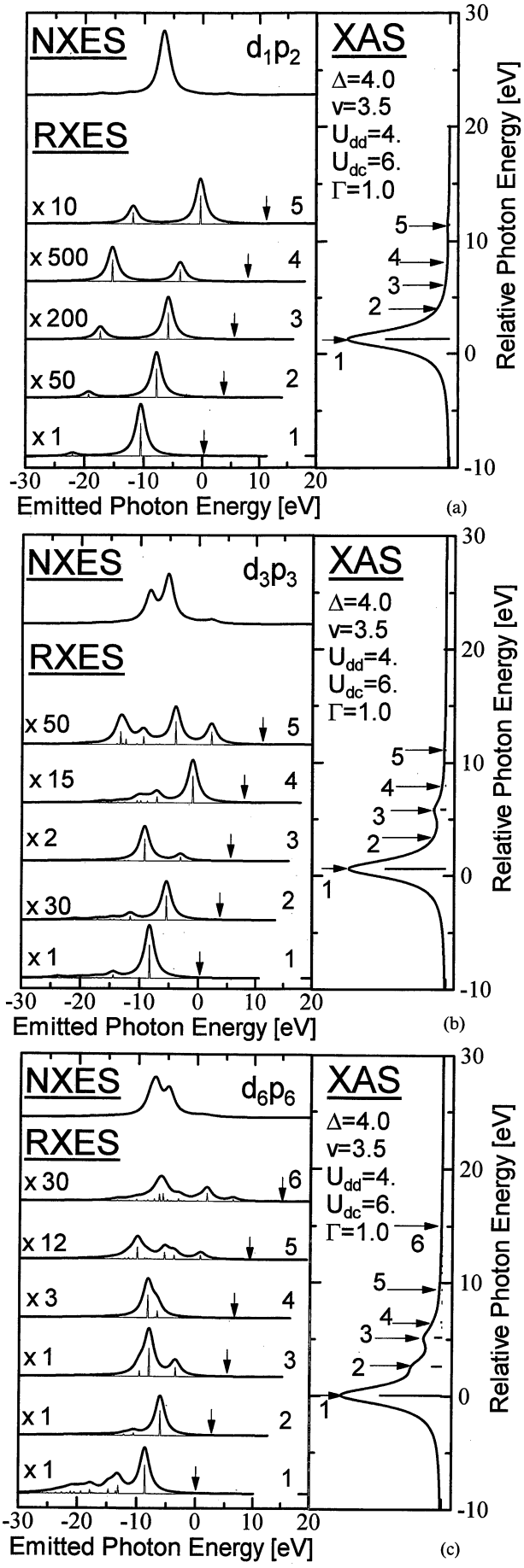

Fig. 3. Calculated XAS and RXES spectra for TiO_2-like parameters with (a) d_1p_2, (b) d_3p_3 and (c) d_6p_6 clusters. NXES spectra are also shown on the top of the RXES curves. Energy positions of the incident photon are indicated by arrows. The magnification rates are also shown as " x 10".

into two peaks for the d_3p_3 cluster, and the relative intensity of the two peaks changes for the d_6p_6 cluster.

3.3 Results for CeO_2-like parameters

Figures 4(a)–4(c) show XAS, RXES and NXES spectra with the CeO_2-like parameters for various sizes of the cluster. We see that the XAS spectra have two-peak structure. The main and satellite peaks correspond, respectively, to the bonding and anti-bonding states between $\underline{c}f^1$ and $\underline{c}f^2\underline{L}$ configurations. The cluster size dependence of XAS is very small, and we only recognize, with increasing cluster size, a slight increase of the spectral intensity in the region between the main peak and the satellite.

The cluster size dependence of RXES for the CeO_2-like system is much smaller than that of the TiO_2-like system, and the energy of the main inelastic scattering feature follows the change of Ω even with large clusters. In the case of the single cluster system f_1p_2, the RXES spectra exhibit a main inelastic scattering peak (corresponding to a single charge transfer excitation), except for the incident photon energy 1, and the peak energy ω shifts in parallel with Ω. With increasing cluster size, this peak is broadened because the corresponding line spectrum shows a fine spectral splitting into some line spectra. Comparing the results for f_1p_2 and f_6p_6 clusters, we see that the single-cation cluster model is a good approximation for describing the RXES except for the incident photon energy 1. On the case 1, some discussion will be given in the next section.

The NXES spectrum with f_1p_2 cluster has two peaks, corresponding to the bonding and anti-bonding states between $f^0\underline{L}$ and $f^1\underline{L}^2$ configurations in the final state. With increasing cluster size, the lower energy peak is more broadened, but we observe much smaller dependence on the cluster size compared with the TiO_2-like system.

§4. Discussion

4.1 Applicability of the sigle-cation-site model

According to Fig. 2, it is found that the cluster size dependence is extremely small for the calculated XPS spectra of both the TiO_2-like and CeO_2-like systems. The XAS spectra shown in Figs. 3 and 4 depend on the cluster size slightly more than XPS, but still the dependence is very small. These suggest that the single-cation-site model can well describe XPS and XAS, which are typical examples of the first-order optical process. So we justify previous theoretical analyses of Ti $2p$XPS and $2p$XAS of TiO_2[9] and Ce $3d$XPS and $3d$XAS of CeO_2[10,11] with a small cluster model or the impurity Anderson model.

For RXES and NXES, on the other hand, it is shown that the cluster size dependence is very important for the TiO_2-like system, while the single-cation-site cluster model works as a fairly good model for the CeO_2-like system. According to the Ti $3d$-$2p$ RXES spectra measured experimentally by Tezuka *et al.*[7] and Butorin *et al.*,[8] strong inelastic scattering spectra whose energy ω do not follow the change of the incident photon energy Ω were observed. These spectra cannot be explained with the single-cation-site model, but are qualitatively consis-

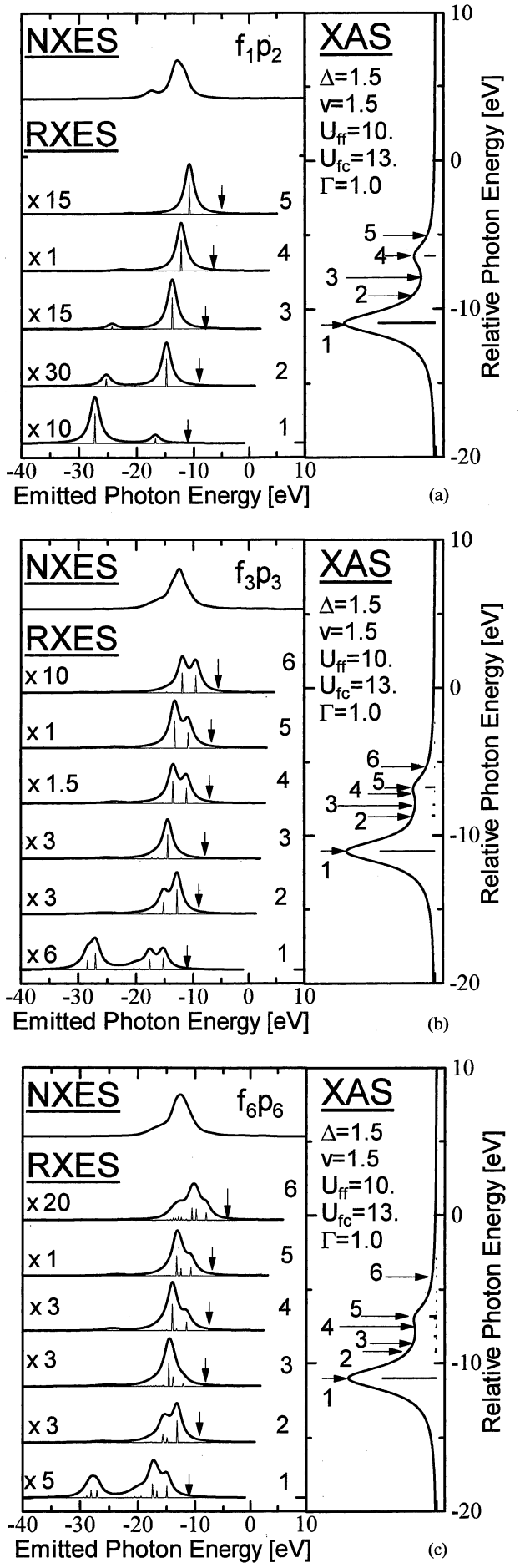

Fig. 4. XAS and RXES spectra for CeO_2-like parameters with (a) f_1p_2, (b) f_3p_3 and (c) f_6p_6 clusters. See the caption for Fig. 3.

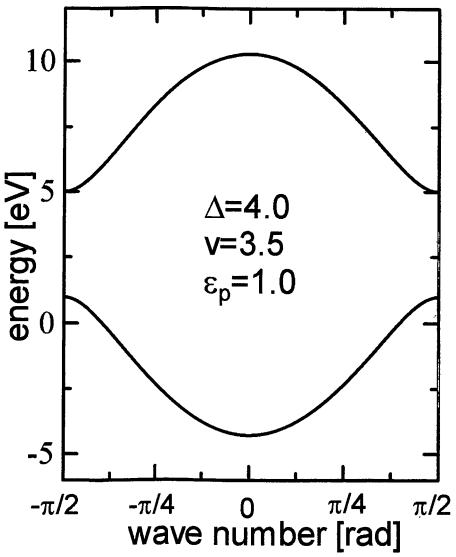

Fig. 5. One electron energy dispersion in the absence of U_{dd} and U_{dc}. Parameters used are indicated in the panel.

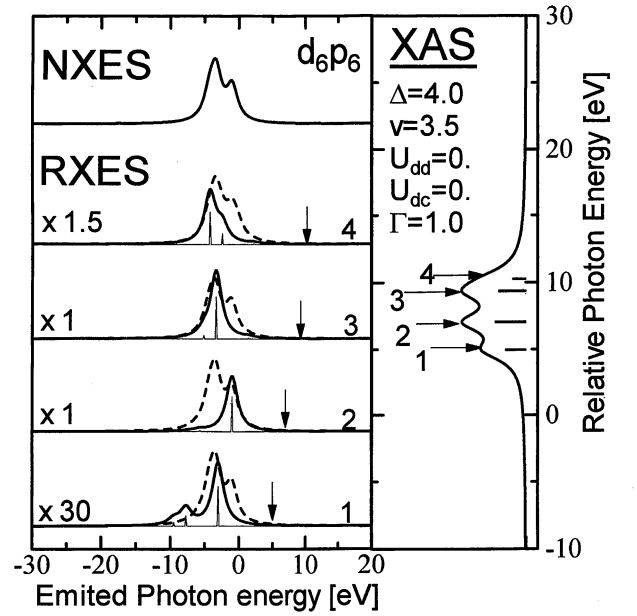

Fig. 6. RXES spectra in the free electron limit $U_{dd} = U_{dc} = 0$ (solid line). Parameters other than U_{dd} and U_{dc} are the same as TiO_2-like ones. Core-fixed RXES spectra are also shown with dashed line. See the caption for Fig. 3.

tent with the NLE spectra calculated here with larger clusters. The mechanism of the cluster size dependence of RXES, especially the NLE spectra in TiO_2, will be discussed in the following subsections.

4.2 NLE spectra in large cluster models

In order to understand the cluster size effect in the TiO_2-like system, it is instructive to study the situation in the limit of $U_{dd} = U_{dc} = 0$. In this case, the initial and final states of RXES are described exactly by one-electron Bloch states with the energy dispersion (Fig. 5):

$$\varepsilon_{\pm}(k) = \varepsilon_p + \frac{\Delta}{2}[1 \pm \sqrt{1 + (4v/\Delta)^2 \cos^2 k}]. \qquad (4.1)$$

RXES spectra for d_6p_6 system in the limit of $U_{dd} = U_{dc} = 0$ (other parameters are taken as the same as those of the TiO_2-like parameters) are shown in Fig. 6. The number of k-points in the first Brillouin zone of the d_6p_6 system is six, i.e. $\{0, \pm\pi/6, \pm 2\pi/6, 3\pi/6\}$, and the number of the excited electron energies is four. In the XAS spectrum of Fig. 6, four peaks are observed in accordance with these four points.

The RXES spectral shape (solid curves) depends on the incident photon energy Ω (but it does not shift in parallel with Ω). This is a result of the k-conservation rule, as Carlisle *et al.* observed and interpreted in graphite.[4] Close inspections show that the inelastic spectra for any excitation energy consists of three lines. These correspond to states with an electron-hole pair in $\{0, \pm\pi/6, \pm 2\pi/6\}$, from lower to higher energy. When Ω resonates with the XAS energies 4, 3 and 2, the excited conduction electron in the intermediate state has mainly the wave numbers $0, \pm\pi/6$ and $\pm 2\pi/6$, respectively, so that the final states of these RXES have an electron-hole pair, where both of the electron and the hole are at $k = 0$, $\pm\pi/6$ and $\pm 2\pi/6$, due to the k-conservation rule. The valence (conduction) band of $k = 3\pi/6$ is pure p-state (d-state) as suggested by eq. (4.1), thus the final state with an electron-hole pair in $3\pi/6$ has no contribution to the RXES spectra within the limit of the intra-atomic transition model (as shown in eq. (2.5)), and the inelastic scattering process is necessarily virtual one for the incident photon energy 1.

If we fix a core hole site in the intermediate state, the k-conservation rule breaks down. RXES spectra calculated with a fixed core hole site are shown in Fig. 6 with dashed curves. In this case the spectral shape of RXES is the same as that of NXES. This is because the excited conduction electron has no contribution to the RXES spectral shape, so that the situation is the same as NXES.

These results suggest the origin of the cluster size effect in the TiO_2-like system. If the cluster size is small, an excited conduction electron is necessarily localized and makes an active contribution to the X-ray emission process. In this case, the emitted photon energy shifts in parallel with the incident photon energy. But when the cluster size is large, we have some intermediate states in which the excited conduction electron state is extended in space as in the case of $U_{dd} = U_{dc} = 0$, then the NLE spectra come arise. The dependence of the NLE spectra on the incident photon energy is expected to come from the k-conservation rule (see §4.3).

Effects of finite values of U_{dd} and U_{dc} are also important in the TiO_2-like system. In order to see the effect of U_{dc}, calculated RXES spectra with $U_{dd} = 0$ but $U_{dc} = 6.0$ eV are shown in Fig. 7. A strong main peak 1 is observed in XAS, which corresponds to a bound state between the core hole and an electron excited from the core level, i.e. the core exiton.[20] Comparison of Fig. 6 and Fig. 7 shows that the RXES spectra are more broadened and exhibit new fine structures as a result of U_{dc}, which causes excitations of more than one electron-hole pairs in the final state, although the final state Hamiltonian is independent of U_{dc}. However, the RXES spectra of 2, 3 and

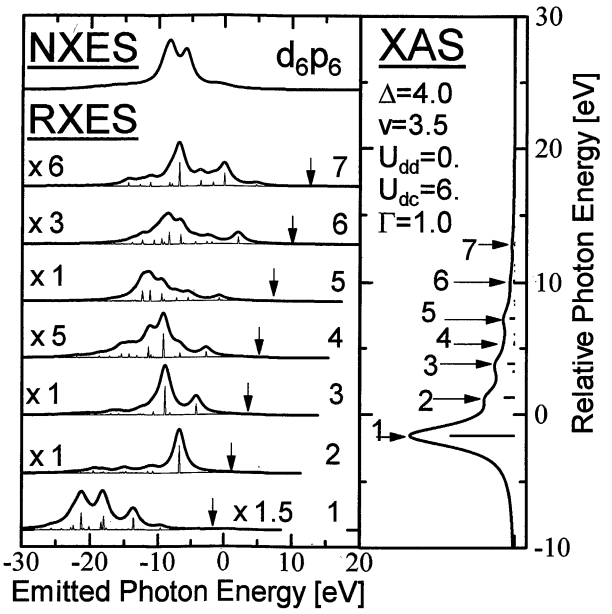

Fig. 7. Role of the core hole potential U_{dc} in RXES spectra. Parameters other than U_{dd} are the same as TiO_2-like ones. See the caption for Fig. 3.

4 in Fig. 7 are found to resemble those in Fig. 6, and this suggests that these intermediate states have somewhat common characters with spatially extended conduction electron states.

It appears that a weak peak located at the highest energy ω shifts in parallel with Ω, but this occurs as a result of the finite size N.

When we introduce a finite value of U_{dd}, occurrence of doubly occupied orbital states is considerably suppressed, and then the RXES in Fig. 7 is changed to that in Fig. 3(c). The RXES spectral broadening in Fig. 7 is somewhat suppressed in Fig. 3(c), because of the suppression of more than one electron hole pairs in the final state. However, the effect of U_{dd} is not very strong except for the case of 1, because the occupation number of d electrons is small in most states of the TiO_2-like system.

Compared with the TiO_2-like system, the cluster size dependence of RXES in CeO_2-like system is much smaller because of the smaller value of the hybridization v.

4.3 Role of the k-conservation rule

To study effects of the k-conservation rule in TiO_2-like and CeO_2-like systems, we calculate RXES spectra by fixing the core orbital on a single site and compare them with those including the translational symmetry of core orbitals (denoted as "coherent spectra"). The results are shown in Fig. 8. The TiO_2-like spectra in Fig. 8(a) show clear difference between the fixed core-site and coherent spectra. The fixed core-site spectra are considerably broader than the coherent ones for the incident photon energy of 2, 3 and 4. This is clearly attributed to the k-nonconserving nature of the fixed core-site model. Thus, the role of k-conservation is (1) to narrow the inelastic peak width, and (2) to fluctuate their peak position around that of NXES spectra.

Note that the RXES spectral shape depends on the incident photon energy even with the core-fixed k-nonconserving model. This is in strong contrast to the case of $U_{dd} = U_{dc} = 0$ (Fig. 6). Because of finite values of U_{dd} and U_{dc}, the photo-excited conduction electron in the intermediate state cannot be a single Bloch state, and some rearrangement between the conduction and valence electron states occurs in going from the intermediate to the final states. Therefore, the origin of the dependence of the NLE spectra on the incident photon energy is partly the effect of the k-conservation rule and partly the effect of U_{dd} and U_{dc}.

According to Fig. 8(b), there is little difference between the fixed core-site and coherent RXES spectra for the CeO_2-like parameters, although close inspections show that we have slightly broader spectral shapes with the fixed core-site model. For the CeO_2-like system, the quasi-particle bandwidth is of the same order as the lifetime in the final state. Furthermore the small value of v/U_{fc} makes the intermediate state almost localized. Then clear cluster size effects are not observed. The fact that the fixed core-site and coherent spectra are almost the same demonstrates the reason why the analyses of Ce $4f$-$3d$ RXES with the impurity Anderson model have successfully reproduced the experimental result.[11]

4.4 Limitation of the present model

We have discussed qualitatively the cluster size effect of RXES in TiO_2 and CeO_2. In order to make more quantitative study, it is necessary to improve the model. Firstly, the atomic arrangement should be improved from the 1D model to more realistic 3D models of TiO_2 and CeO_2. Secondly, the orbital degeneracies of d (or f) and p states should be taken into account. As shown in the Appendix, we have introduced the effective hybridization v, in which effects of orbital degeneracies on the hybridization between d^0 and $d^1\underline{L}$ are taken into account. With this effective hybridization, however, effects of orbital degeneracies on the hybridization between $\underline{c}d^1$ and $\underline{c}d^2\underline{L}$ configurations in the intermediate state cannot be well described. Furthermore, the effects of orbital degeneracies are essential in the calculation of RXES for the incident photon energy tuned to the main XAS peak 1. As shown by Nakazawa *et al.*,[11] the main inelastic RXES spectra in the resonance with the XAS main peak of CeO_2 originate from the nonbonding $d^1\underline{L}$ final states, instead of the antibonding state between d^0 and $d^1\underline{L}$ configurations. The nonbonding final states occur only by taking explicitly into account the orbital degeneracies. The situation is also the same for TiO_2. In this sense, the present calculation of RXES for the case 1 is not realistic. More realistic calculations with an improved model is left for future investigations.

§5. Conclusions

We have numerically studied multi-cluster effects on XPS, XAS, NXES and RXES spectra. The model we have used is that which describes qualitatively these spectra for TiO_2 and CeO_2. Following results have been obtained.

Firstly, we showed that the cluster size dependence is

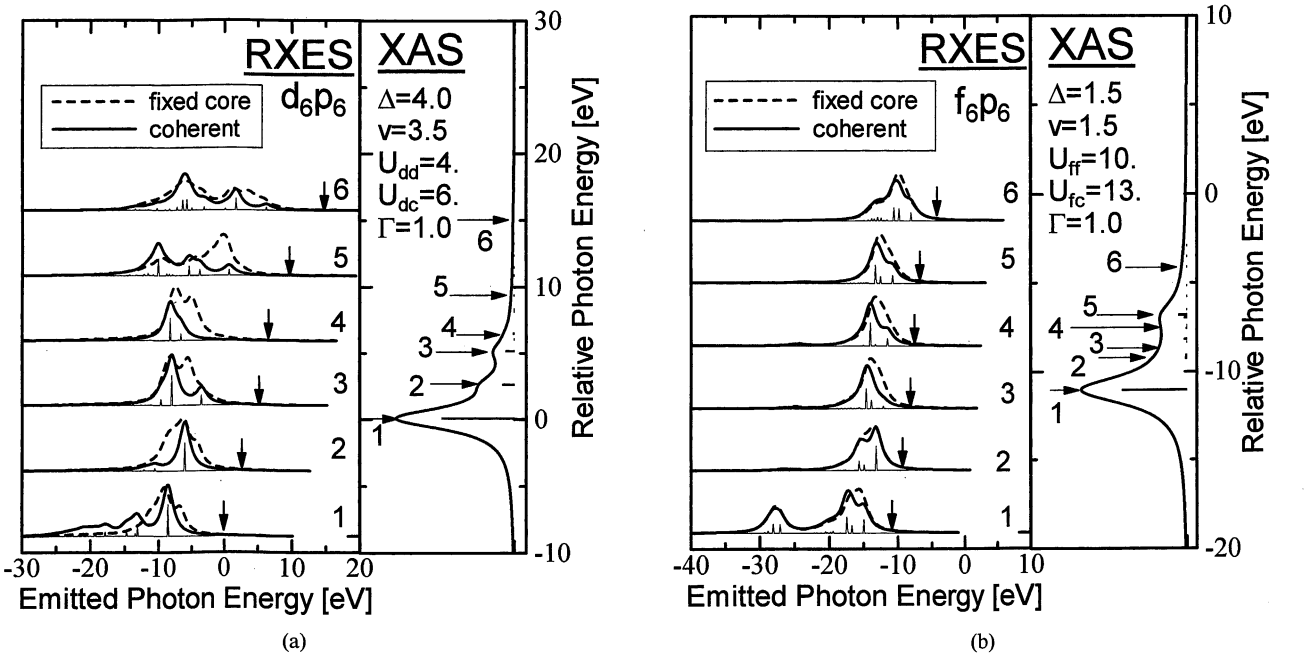

Fig. 8. Comparison between fixed core-site and coherent calculations of RXES spectra for (a) TiO_2-like and (b) CeO_2-like systems with six unit clusters. The fixed core-site spectra are represented with dashed line, and the coherent ones with solid line. See the caption for Fig. 3.

extremely suppressed for the first order optical process, XPS and XAS. It suggests that the impurity model is applicable to the analysis of these spectra, in contrast to the second-order optical process, RXES and NXES.

Secondly, for the TiO_2-like parameters, we numerically demonstrated the occurrence of NLE spectra as a result of the multi-cluster effect. The behavior of NLE spectra is qualitatively consistent with the Ti $3d$-$2p$ RXES experiment of TiO_2. The origin of NLE spectra is the occurrence of spatially extended conduction electron states in the intermediate state of large clusters. The dependence of NLE spectra on the incident photon energy originates from the k-conservation rule, as well as from the effects of U_{dd} and U_{dc}.

Thirdly, for the CeO_2-like system we have shown that the multi-cluster effects in RXES spectra are fairly suppressed, compared with the TiO_2-like system, because of the smaller hybridization strength v. The effect of large clusters is the broadening of inelastic peaks.

Finally we should take into account the effect of orbital degeneracies for more quantitative study of cluster size effect of RXES in TiO_2 and CeO_2.

Acknowledgements

The authors would like to express their thanks to Professor K. Okada and Professor S. Tanaka for their valuable discussion. This work is partly supported by a Grant-in-Aid for Scientific Research from the Ministry of Education, Science, Sports and Culture. The computation in this work was done using the facilities of the Super-Computer Center, Institute for Solid State Physics, University of Tokyo.

Appendix: Effective Hybridization

In the TiO_6 cluster model with the local O_h symmetry and with full orbital degeneracies, the Hamiltonian of hybridization between Ti $3d$ orbitals and O $2p$ ligand molecular orbitals is given by

$$H_1' = \sum_{\Gamma,m,\sigma} \left[V(\Gamma)\, d^\dagger_{\Gamma m\sigma} p_{\Gamma m\sigma} + \text{H.c.} \right], \qquad \text{(A·1)}$$

where Γ runs over two irreducible representations of O_h, i.e. e_g and t_{2g}, and m distinguishes the 2- or 3-fold degeneracies of them. On the other hand, in the single cluster limit (Fig. 1(a)), the hopping energy of our model satisfies $2v = \langle d^0|H|d^1\underline{L}\rangle$, where $|d^0\rangle = p^\dagger_\uparrow p^\dagger_\downarrow|0\rangle$ and $|d^1\underline{L}\rangle = \frac{1}{\sqrt{2}}\sum_\sigma d^\dagger_\sigma p_\sigma |d^0\rangle$ with the ligand state $p_\sigma = \frac{1}{\sqrt{2}}(p_{1\sigma}+p_{2\sigma})$. $|0\rangle$ denotes the state which has no valence electrons but has filled core levels.

Now we map the hybridization strength of TiO_6 cluster onto 1D d-p model. It is quite natural to define our v as

$$2v \equiv \max\{\langle d^0|H_1'|d^1\underline{L}\rangle\}, \qquad \text{(A·2)}$$

where $|d^1\underline{L}\rangle$ is a linear combination such as

$$|d^1\underline{L}\rangle = \sum_{\Gamma,m,\sigma} \alpha_{\Gamma m\sigma} d^\dagger_{\Gamma m\sigma} p_{\Gamma m\sigma}|d^0\rangle, \qquad \text{(A·3)}$$

and the coefficients $\{\alpha_{\Gamma m\sigma}\}$ are chosen to maximize $\langle d^0|H_1'|d^1\underline{L}\rangle$ under the normalization condition $\sum_{\Gamma,m,\sigma}\alpha^2_{\Gamma m\sigma} = 1$.

It is easy to solve the extremum problem and show that the effective hybridization defined by eq. (A·2) is given by

$$v = \frac{1}{2}\sqrt{4V(e_g)^2 + 6V(t_{2g})^2} \qquad \text{(A·4)}$$

for

$$\alpha_{\Gamma m\sigma} = \frac{V(\Gamma)}{\sqrt{6V(t_{2g})^2 + 4V(e_g)^2}}. \qquad \text{(A·5)}$$

In the case of the CeO_2-like system, we can take

$$H_1' = V \sum_{m,\sigma} \left[f_{m\sigma}^{\dagger} p_{m\sigma} + \text{H.c.} \right] \qquad \text{(A·6)}$$

with $SO(3)$ symmetry and 7-fold degeneracy of $l = 3$ orbital. Therefore, the effective hybridization v is given by

$$v = \frac{\sqrt{14}}{2} V. \qquad \text{(A·7)}$$

1) See for example, S. Hüfner: *Photoelectron Spectroscopy*, Springer; F. M. F. de Groot: J. Electron. Spectrosc. Relat. Phenom. **67** (1994) 529.
2) M. van Veenendaal and G. A. Sawatzky: Phys. Rev. Lett. **70** (1993) 2459.
3) M. van Veenendaal, H. Eskes and G. A. Sawatzky: Phys. Rev. B **47** (1993) 11462; M. van Veenendaal and G. A. Sawatzky: Phys. Rev. B **49** (1994) 3473; K. Okada and A. Kotani: Phys. Rev. B **52** (1995) 4794.
4) J. A. Carlisle, Eric L. Shirley, E. A. Hudson, L. J. Terminello, T. A. Callcott, J. J. Jia, D. L. Ederer, R. C. C. Perera and F. J. Himpsel: Phys. Rev. Lett. **74** (1995) 1234.
5) J.-E. Rubensson, D. Mueller, R. Shuker, D. L. Ederer, C. H. Zhang, J. Jia and T. A. Callcott: Phys. Rev. Lett. **64** (1990) 1047.
6) Y. Ma, N. Wassdahl, P. Skytt, J. Guo, J. Nordgren, P. D. Johnson, J-E. Rubensson, T. Boske, W. Eberhardt and S. D. Kevan: Phys. Rev. Lett. **69** (1992) 2598.
7) Y. Tezuka, S. Shin, A. Agui, M. Fujisawa and T. Ishii: J. Phys. Soc. Jpn. **65** (1996) 312.
8) S. M. Butorin, J.-H. Guo, M. Magnuson and J. Nordgren: Phys. Rev. B **55** (1997) 4242.
9) K. Okada and A. Kotani: J. Electron Spectrosc. Relat. Phenom. **62** (1993) 131.
10) T. Jo and A. Kotani: J. Phys. Soc. Jpn. **55** (1986) 2457.
11) M. Nakazawa, S. Tanaka, T. Uozumi and A. Kotani: J. Phys. Soc. Jpn. **65** (1996) 2303.
12) Here we have disregarded the geometrical (angular dependent) factor. In realistic three dimensional systems it is quite important for understanding experimental RXES spectra. For effects of the angular dependence on RXES, see, *e.g.*, F. M. F. de Groot, M. Nakazawa, A. Kotani, M. H. Krish and F. Sette: Phys. Rev. B **56** (1997) 7285.
13) T. Minami and K. Nasu: Phys. Rev. B **57** (1998) 12084.
14) Y. Ma: Phys. Rev. B **49** (1994) 5799.
15) K. E. Miyano, D. L. Ederer, T. A. Callcott, W. L. O'Brien, J. J. Jia, L. Zhou, Q.-Y. Dong, Y. Ma, J. C. Woicik and D. R. Mueller: Phys. Rev. B **48** (1993) 1918.
16) M. van Veenendaal and P. Carra: Phys. Rev. Lett. **78** (1997) 2839.
17) J. D. Jackson: *Classical Electrodynamics* (John Wiley and Sons, NY), 2nd. ed. Chap. 9.
18) E. Dagotto: Rev. Mod. Phys. **66** (1994) 763.
19) R. Barrett, M. Berry, T. F. Chan, J. Demmel, J. Donato, J. Dongarra, V. Eijkhout, R. Pozo, C. Romine and H. van der Vorst: *Templates for the Solution of Linear Systems: Building Blocks for Iterative Methods*, Society for Industrial and Applied Mathematics, 1994.
20) R. J. Elliott: Phys. Rev. **108** (1957) 1384, and references therein.